

Supplemental Figures

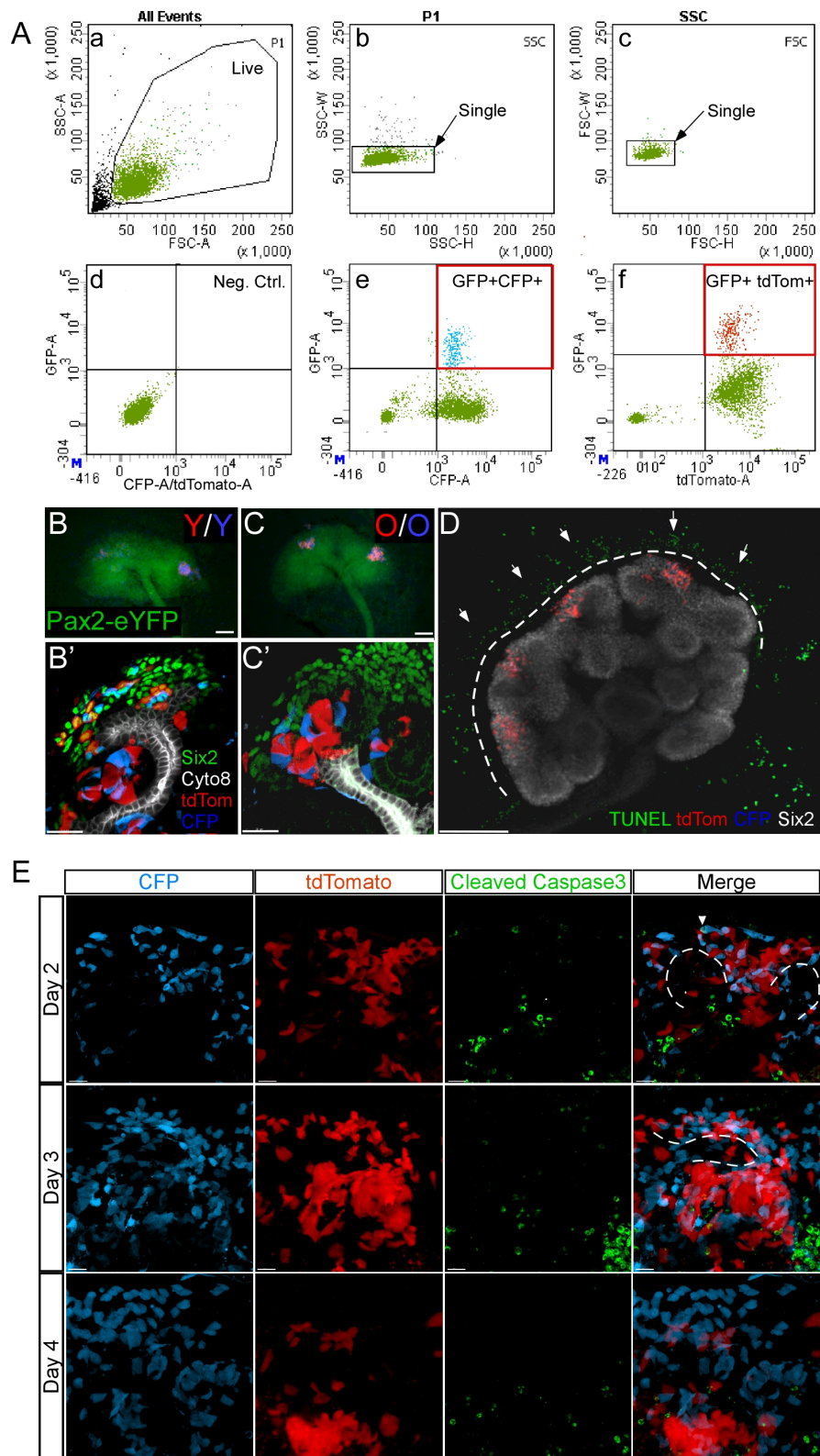


Figure S1 (related to Figure 1 and 2). (A) The gating steps applied to sort the progenitors. Live cells identified by forward and side scatter (a). Single cells were selected in two steps based on their size in the forward and side scatter (b and c). Cells that were selected for injection if they were CFP+/GFP+ (e) or tdTomato+/GFP+ (f) from the quadrant outlined in red (d - negative control). (B-C) Double positive progenitors collected from (e) and (f) were transplanted into the CM niche of E12.5 Pax2-eYFP recipient kidney at 1:1 mixture (in B-B', E12.5 red vs. E12.5 blue; in C- C' P0 red vs. P0 blue). Injection of transplanted cells into the CM is visualized using the Pax2-eYFP reporter that marks nephron progenitors and the ureteric bud. (B'-C') Representative image showing immunostaining of injected explants after 4-days of ex-vivo culturing. Six2 antibody (green) marks nuclei in the CM and Cytokeratin8 (white) labels the UB cells. Note that red and blue cells behaved similarly if they came from the same age donor (B' and C') and a majority of the P0 cells exit the niche in C'. (D). TUNEL staining detected apoptotic cells outside of the kidney anlagen (arrows) but not inside the kidney (dotted line). (E) Immunostaining of three injection points at the end of day 2, 3 and 4 after injection respectively. Cleaved caspase-3 (green) marks cells undergoing apoptosis. UB is marked by dotted white line. Note very little overlap of cleaved caspase-3 with injected nephron progenitors. Scale bars in (B-C) 1mm, (B'-C') 30µm, (D) 200µm and (E) 15 µm.

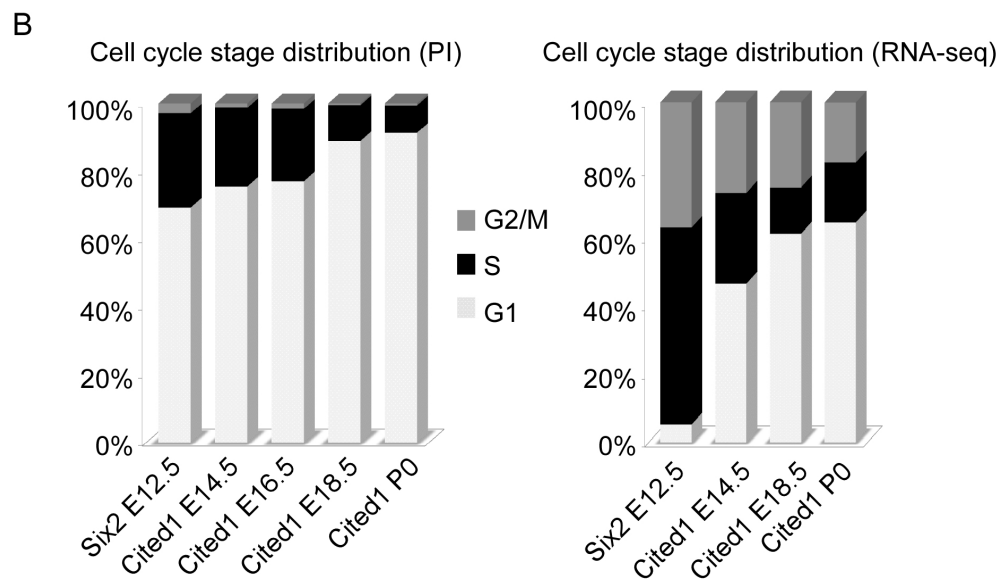
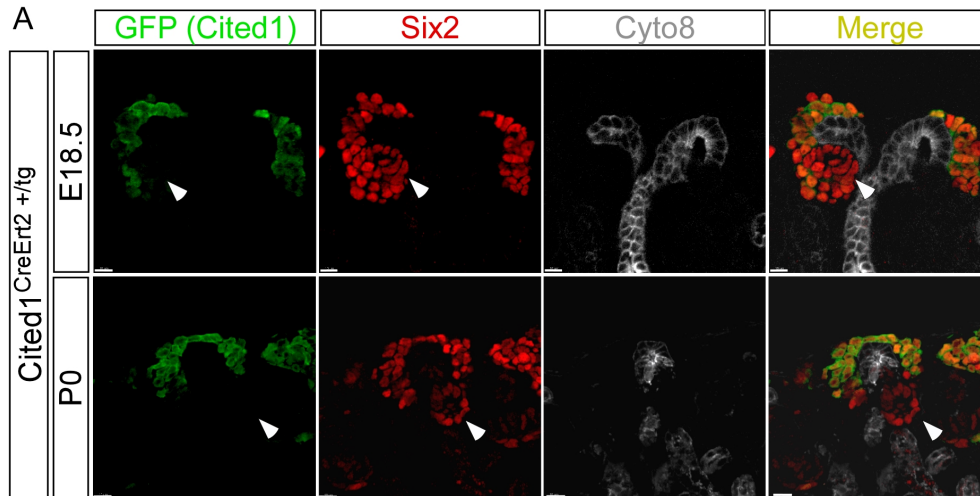


Figure S2 (related to Figure 3). (A) Antibody staining of GFP (green, reporting Cited1+) labeled a more distal population of nephron progenitors than Six2 (red). Note that only Six2 is detected in the PTA. Cytokeratin8 (Cyto8) labeled the UB. Scale bar, 10 μ m. (B) Analysis of cell cycle stage distribution of nephron progenitors based on propidium iodide staining (left) and cyclin/CDK expression profile from single cell RNA-seq (right). Note that gene expression profiling did not capture the length of G1 but did capture the proportional change in S,G2,M.

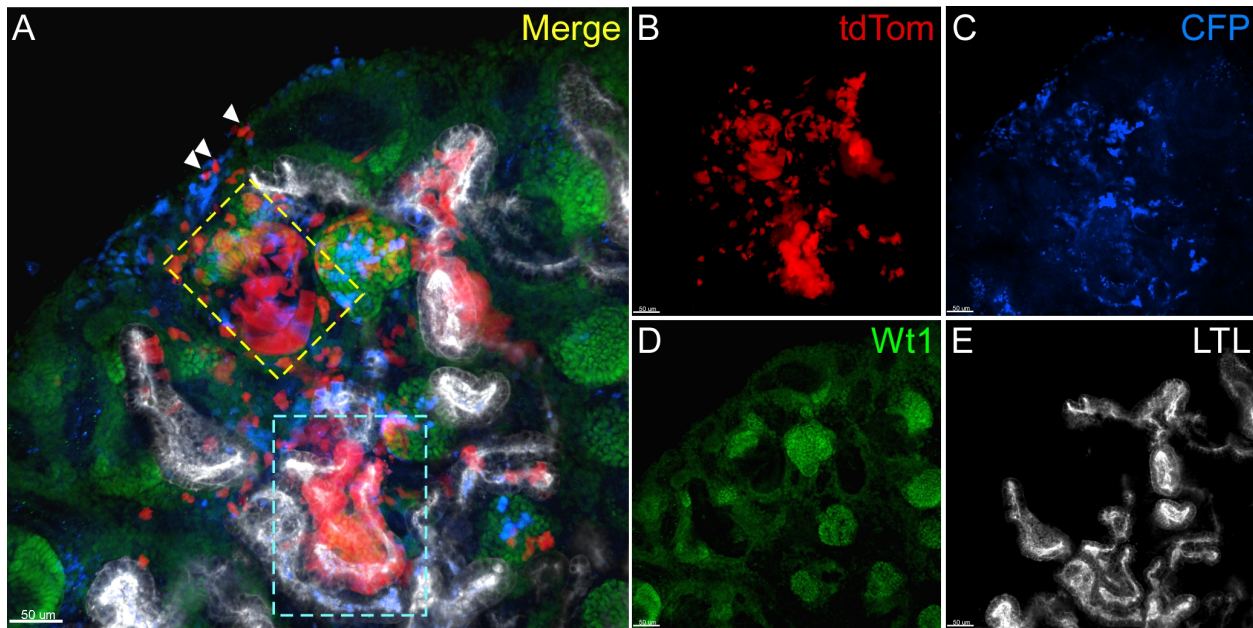


Figure S3. Old progenitors remaining the CM actively contribute to nephron formation (related to Figure 4). (A-E) antibody staining of injected metanephroi cultured for 7 days. E12.5 (Blue) and P0 (Red) were both found in the CM (weak green, Wt1 labeling), a newly forming S-Shaped body (yellow dotted box) and more mature proximal tubule segment (white, LTL, Cyan dotted box). Scale bar, 50 μ m. (F-G) Quantification of the percentage of “single” Six2⁺ (F) and Cited1⁺ (G) cells to total cells in a niche by the end of 4-day culture in 37 injected niches. Note that increasing the neighboring cell distance criteria from 12 μ m to 15 μ m showed similar results (compare to Figures 4G-H).

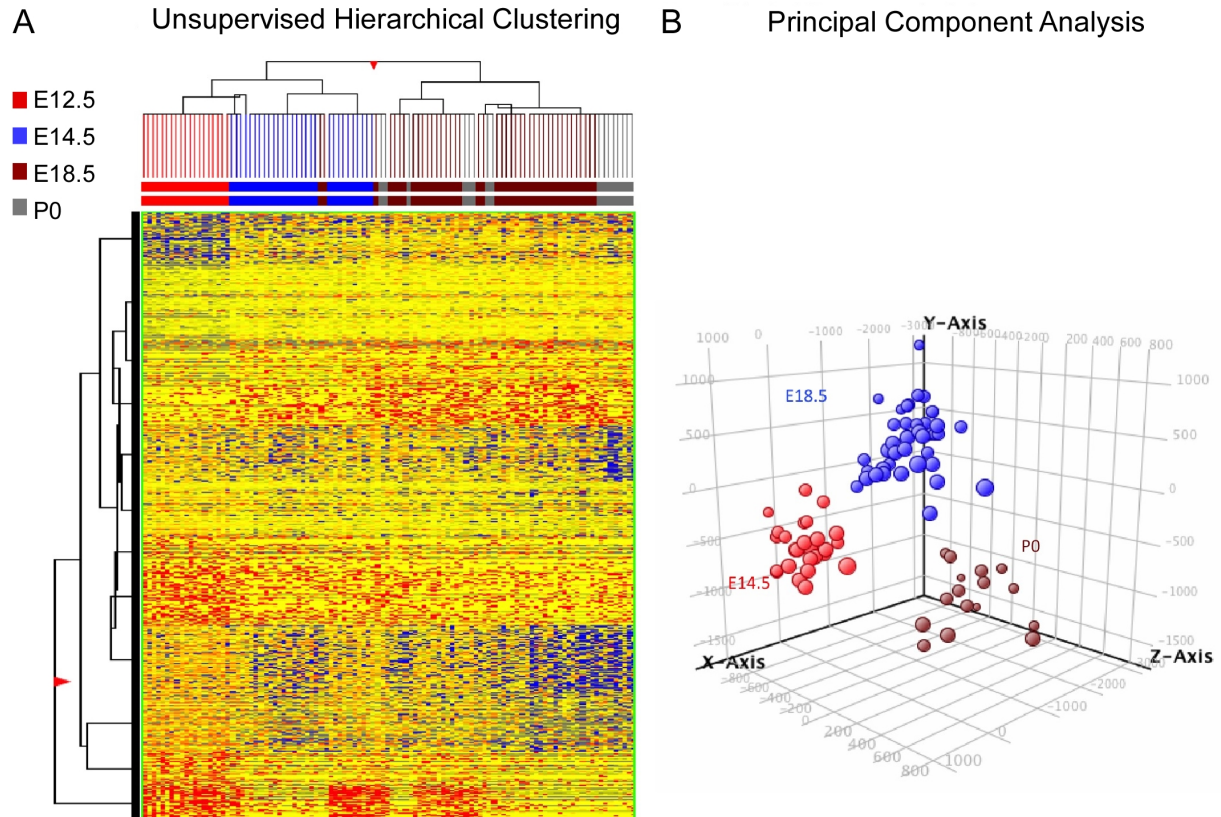


Figure S4 (related to Figure 7). Single cell RNA-seq analysis of Cited1+ progenitors. (A) A heat map depicting the expression of genes in Cited1+ progenitors isolated from E12.5, E14.5, E18.5 and P0 kidneys. Unsupervised clustering was performed using self-organizing maps (SOM) to visualize the expression patterns of genes (E12.5; Red, E14.5; blue, E18.5, brown, P0; gray). The color intensities red, blue and yellow of the heat map indicate high, low and intermediate expression levels, respectively. (B) Analysis of one-plate, single-cell RNA-Seq data using principle component analysis (PCA) (E14.5, red; E18.5, blue; P0, brown). For further details, consult with Table S2.

Supplemental Tables S1-S7

Provided as downloadable Excel sheets

Table S1 (related to Figure 4). This excel sheet contains the "single" vs "cluster" distribution of old cells by the end of 4 day after injection. Sheet "all data points" contains all 37 injection points from Six2 E12.5 vs. P0 injection as well as all 37 injections points from Six2 E12.5 vs.

Cited1 P0 co-injection. Each injection is identified by the injection date, injection point, age and genotype (Six2 or Cited1) of the cells injected and the percentage of cells that are single with a cut of 12um or 15um. The next sheet includes all data points except those with less than 4 cells. This filtered data sheet is used for the statistical analysis in the last sheet.

Table S2 (related to Figure 7). This excel spreadsheet incorporates single-cell RNA-seq data based on expression markers from e14.5, e18.5 and P0 renal progenitors (Cited1-positive cells). The single-cell data from this study and the selected cells were filtered using a cut-off requiring gene expression present in 10 out of 174 cells and at expression threshold of >5 RPKM. The subsequent gene list was then filtered using a one-way ANOVA p (Corr) 0.05 and a Benjamini-Hochberg Multiple Testing Correction, followed by 6-fold gene expression difference between samples. This filtering paradigm yielded a gene list of 1928 genes.

Table S3 (related to Figure 7). This excel spreadsheet incorporates single-cell RNA-seq data based on expression markers from e12.5 renal progenitors (Cited1-positive cells), e12.5 stromal cells (Foxd1-positive) and P4 renal vesicle cells. The single-cell data from this study and the selected cells were filtered using a cut-off requiring gene expression present in 10 out of 174 cells and at expression threshold of >5 RPKM. The subsequent gene list was then filtered using a one-way ANOVA p(Corr) 0.05 and a Benjamini-Hochberg Multiple Testing Correction, followed by 6-fold gene expression difference between samples. This filtering paradigm yielded a gene list of 910 genes.

Table S4 (related to Figure 7). Sheet 1 includes 328 genes Monocle singled out during analysis. Each Row contains one gene with the Ensemble gene identifier in column A followed by the gene symbol. The p-value and q-value statistical information used for ordering the clusters are included. Sheet 2 contains functional analysis of the 328 genes with ToppGene (related to Figure 7). The ToppGene tool (<http://toppgene.cchmc.org/>) with FDR correction cut off set to 0.05. Top molecular functions, biological processes, and cellular components, along with associated genes, are presented. In addition, human phenotypes, mouse phenotypes, domains, pathways and diseases are listed. The best candidate regulatory transcription factors, candidate target genes, as well as regulatory microRNAs and candidate target genes, are listed.

Table S5 (related to Figure 7). This excel sheet contains a graphical representation of the 12 K-means clusters identified using the self-organizing map (SOM) unsupervised clustering. The top affiliated GO-terms for each cluster is included along with p-values. Refer to accompanying K-means cluster list for the full list of GO-terms and gene lists.

Table S6 (related to Figure 7). Each Excel sheet contains the individual gene lists from 12 K-means clusters generated using the unsupervised self-organizing map (SOM) clustering algorithm in the analysis of 1928 Anova Gene list in this study.

Table S7 (related to Figure 7). Each of the 12 K-means cluster was analyzed using the ToppGene tool (<http://toppgene.cchmc.org>) with the following settings: FDP correction with a p-value cut-off of 0.05. Top molecular functions, biological processes and cellular components, along with associated genes, are presented. In addition, human phenotypes, mouse phenotypes, domains, pathways and diseases are listed. The best candidate regulatory transcription factors, along with candidate target genes, as well as regulatory microRNAs are listed.

Supplemental Experimental Procedures

Animals

The starting colony for this experiment include the following lines: *Six2*^{TGC +/tg} (Kobayashi et al., 2008), *Rosa*^{Ai9/Ai9} [or *Rosa*^{tdTom/tdTom}, (Madisen et al., 2009)], *CAG-eCFP*^{tg/tg} (Hadjantonakis et al., 2002), *Rosa*^{eYFP/eYFP} (generated by Frank Costantini, Columbia University, obtained from JAX), *Cited1*^{CreErt2GFP +/tg} (Boyle et al., 2008), *Pax2*^{Cre +/tg} (Ohyama and Groves, 2004), *Fgf20*^{βGal/βGal} (Huh et al., 2012, referred to as *Fgf20*^{-/-}) and the constitutively activated version of *Rosa*^{tdTom/tdTom}, *Rosa*^{Tom-A/Tom-A}, where the stop codon were floxed-out by mating male *Rosa*^{tdTom/tdTom} with female *Msx2*^{Cre+/tg}. In order to obtain embryos with different transgenic reporters of different ages on the same experiment day, we generated the males of the following genotypes: *Six2*^{TGC +/tg}; *Rosa*^{tdTom/tdTom}, *Six2*^{TGC+/tg}; *CAG-eCFP*^{tg/tg}, *Cited1*^{CreErt2GFP +/tg}; *Rosa*^{tdToma-A/tdTom-A}, *Cited1*^{CreErt2GFP +/tg}; *CAG-eCFP*^{tg/tg}. These males are then used to set up time mating with CD1 females at the pre-estrous or estrous stage. *Pax2*^{Cre +/tg} males are mated with *Rosa*^{eYFP/eYFP} to generate *Pax2*^{Cre +/tg}; *Rosa*^{+eYFP} animals.

FACS sorting of nephron progenitors

E12.5, E14.5, E18.5 and P0 kidneys were dissected from control (no transgene) or Six2TGC+/tg or Cited1CreERT2+/tg mice containing either Rosa tdTomato or Actin-CFP reporter and placed into ice cold PBS. After removal of PBS, TrypLE (Invitrogen, 12604-013) solution was added to dissociate the kidneys. To facilitate the dissociation process, kidneys older than E18.5 were cut into smaller pieces with a razor blade and triturated with progressively smaller pipette tips (p1000- p10) during its 15min incubation on ice. When no large clumps were visible, enzyme digestion was stopped by addition of kidney media containing 10% FBS. The dissociated cells were filtered through 40um cell strainer (352340, Falcon) and spun down for 5min at 500G. Following media aspiration, cell pellets were resuspended in appropriate volumes of FACS buffer (PBS with 3% FBS) and kept on ice until FACS sorting. Sorting was performed by BD FACSDiva flow cytometer. Gating was implemented based on negative control profiles to select for live, single cell that was GFP+tdTomato+ or GFP+CFP+ double positive. Sorted cells were collected in 1.7 ml eppendorf tubes containing 900ul of kidney media with 5% FBS and kept on ice before plating. Finally, cells were spun down for 5 min at 500G in a 15ml conical tube in a swing-bucket centrifuge and resuspended into 20ul before being plated on trans-well filters in organ culture dishes.

Preparation of glass capillary needles for transplantation

Glass capillaries (TW-100, World Precision Instruments) were cleaned with acetone (4hrs- on shaker), 100% ethanol (4hrs- on shaker), deionized water (soak overnight followed by flowing 30ml of autoclaved dH₂O through each capillary tube) and allowed to dry overnight in an oven (80 °C). Clean glass capillaries were pulled with a Flaming/Brown type micropipette puller (P-97, Sutter Instrument) with a heat of 820, pull force of 150, velocity of 150 and a time/delay of 150. Using the needle-on-needle method (Pipette cookbook, Sutter) the needles were further trimmed to have an opening of 25-35um at the needle tip (measured with a micrometer). Trimmed needles were fire-polished at the tip with a micro-forge (MF-900, Narishige) at heat level 60 for 2 X 1sec. To prevent cells from sticking to the wall of the needle, the needle tip were either silanized in Sigmacote (SL2 Sigma) for at least 2hrs at room temperature and followed by 3 times washes in H₂O, 70% ethanol and H₂O or coated with 1% BSA for 10min right before injection and washed off with kidney media. To ensure sterility, needles were autoclaved before BSA coating or after silanization.

Transplantation of nephron progenitors

E12.5 recipient kidneys (*Pax2*^{Cre+/tg}; *Rosa*^{+eYFP}) were dissected prior to FACS sorting and cultured as previously described (Barak and Boyle, 2011) until ready to be injected. The injection set includes a fluorescent stereomicroscope (Leica, FM-10), a manual microinjector (IM-6, Narishige) and a

micromanipulator (Narishige) for holding and adjusting the position of the microinjector. To perform the injection, a capillary needle was loaded onto the microinjector and backfilled with H₂O from the injector reservoir to the point where the needle starts to taper. To load FACS purified progenitors into the needle, a negative pressure was applied to take up FACS sorted cells concentrated on the trans-well filter until the media surface came close to the H₂O surface, leaving a small air bubble in between. Once inside the needle, progenitors aggregate at the air-liquid interface at the air bubble, minimizing the amount of liquid in between cells. By gradually applying a positive pressure, concentrated progenitors are pushed towards the tip of the capillary and injected into the CM niche of recipient kidneys using the eYFP fluorescence as a guide. Each metanephroi were injected at 2-4 different niche locations. Injected kidneys were then cultured for another 4-7 days with media changed once every 24hrs.

Antibodies used for immunostaining

Primary antibodies used include Six2 (1:300, 11562-1-AP, Proteintech), Cytokeratin 8 (1:50, Troma-1, Hybridoma Bank), LTL-Biotin (1:300, B-1325, Vector Lab), ECad (1:300, 610182, Transduction Lab), Wt1 (1:250, sc-192, Santa Cruz Biotechnology.) and PDGFRb (1:500, Affymetrix/eBioscience).

EdU pulse-labeling

EdU stock solution (1mg/ml in PBS) is added to the media to reach a final concentration of 10 μ M at the end of 24 or 48hrs post-injection. Pulse labeling is allowed to last for 3hrs before fixation of culture 4% PFA on ice for 2hrs. Cells are then stained for EdU incorporation according to the Click-iT[®] EdU imaging kit protocol (Life Technologies, C10338) and followed by antibody labeling of Six2. Staining with an incomplete kit on EdU-containing cells was included as negative controls.

Cell cycle analysis with propidium iodide staining

Six2 or Cited1 nephron progenitors were FACS sorted from embryos of multiple litters (E12.5 and E14.5) or multiple embryos from the same litter (E18.5 and P0), n=3. Cells were fixed in pre-chilled methanol (-20°C) overnight and stained with propidium iodide/RNaseA for 30min at 37°C in dark before loading into BD Fortessa II for DNA content based cell cycle analysis. Cell cycle distributions were analyzed with ModFit[™].

Single cell RNA sequencing

We FACS-purified single Cited1⁺ cells isolated from E14.5 (GFP⁺), E18.5 (GFP+tdTomato⁺), and P0 (GFP+CFP⁺) progenitors as we did for the injection. Sequencing libraries generated 3-4 million reads per cell from a total of 91 nephron progenitors cells. Post-hoc sequence analysis of the fluorescent proteins

identified 28 E14.5 GFP+ cells, 47 E18.5 GFP+tdTomato+ cells and 16 GFP+CFP+ P0 cells. To extend our analysis to E12.5 nephron progenitors we incorporated single-cell RNA-seq data derived from E12.5 Cited1+Six2+ nephron progenitors from whole kidneys (Brunskill et al., 2014) (Figure S4A and Table S2). To analyze sequencing data, Bam files from each cell were loaded into Genespring and single-cell data was normalized using DeSeq normalization algorithm. In some instances, the RNA-Seq data was further filtered using a one-way ANOVA p-value cut-off of 0.05 without multiple testing correction.

Mathematical modeling of the nephron progenitor cells

Model construction. The cell number in the niche increases when cells undergo proliferation and decreases when cells undergo cell death or exit. If we assume the proliferation, exit and death rates are all proportional to the cell number (x), then the differential equation describing the cell number can be written as

$$\frac{dx}{dt} = (k_{pr} - k_d - k_e) * x = k * x.$$

Available data from our study and the literature. Not much cell death is observed within the niche during the 4-day culture of nephron progenitor cells, hence a small, negligible death rate (in current study, $k_d=10^{-6} \text{ hr}^{-1}$) can be assigned to all the cells. The proliferation rates (k_{pr}) of nephron progenitor cells have been calculated by Short et al (Short et al., 2014). Although cap mesenchyme cells are heterogeneous, with some cells cycling faster than others, Short et al correctly pointed out that the net proliferation of the cell population could be described with an average proliferation rate. The average proliferation rate is about 1.17 day^{-1} for 13.5dpc cells (whose average cell cycle time is around 14.2 hours (0.59 days)) and about 0.5 day^{-1} for 17.25dpc cells (whose average cell cycle time is around 32.8 hours (1.37 days)), (Sup. Table S1 in Short et al). Based on their estimation, and the observation that older cell proliferate more slowly, we could assign the proliferation rates with the assumption that after E16.5 all cells proliferate at the same average rate (1.17 day^{-1} for Six2-E12.5 cells; 0.5 day^{-1} for Cited1-18.5 and Cited1-P0 cells). We did not assign the rate for E14.5 days since it was not measured.

Estimating the rates based on ratios. The initial injected cell numbers were not captured. The ratios of injected cells at the start were 50/50. Ratios at endpoint were recorded and were highly reproducible, correlating well with the age of the injected population. Hence, we can carry out an analysis on the basis of ratios. We can solve the differential equation

$$\frac{dx}{dt} = k * x$$

To obtain the solution: $x_t = x_0 * e^{kt}$.

If x is used for E12.5 Six2 cells and y for Cited1 cells, we can see that

$$\frac{x_t}{y_t} = \frac{x_0}{y_0} * e^{(k_x - k_y) * t}$$

And because the same number of Six2 and Cited1 cells were injected ($x_0=y_0$):

$$\ln\left(\frac{x_t}{y_t}\right) = (k_x - k_y) * t,$$

Remember that $k = k_{pr} - k_{exit} - k_d$, with k_d being negligible.

Test 1: assume all cell have identical exit rates. In this case we will have

$$\ln\left(\frac{x_t}{y_t}\right) = (k_{prx} - k_{pry}) * t.$$

Given that E12.5 Six2 cells have a $K_{prx} = 1.17 \text{ day}^{-1}$ we can predict the proliferation rate of Cited1 cells based on the observed ratios after four days of culture:

Predicting Proliferation rates based on the assumption that exit rates are fixed:

<u>Cited1 age</u>	<u>xt/yt (Six2/Cited1)</u>	<u>Ln(xt/yt)</u>	<u>Ln(xt/yt)*1/4</u>	<u>$K_{pry} = 1.17 - \text{Ln}(xt/yt) * 1/4$</u>
14.5	35/65=0.54	-0.62	-0.155	1.325
18.5	55/45=1.22	0.2	0.05	1.12
P0	73/27=2.7	1	0.25	0.92

The predicted cell cycle times (CCT) of Cited1 cells at different ages:

<u>Cited1 age</u>	<u>$K_{pry} (\text{day}^{-1})$</u>	<u>CCT (day)</u>	<u>CCT (hour)</u>	<u>Observed CCT (hours)</u>
14.5	1.325	0.523	12.6	?
18.5	1.12	0.619	14.8	32.8
P0	0.92	0.7853	18.1	≥ 32.8

- **Conclusion 1:** If the exit rate is fixed in cells of different ages, then the change of cell proliferation will be the only mechanism driving the observed changes in cell number. The rates obtained by the model do not agree with the observed rates (Short et al) indicating that the assumption of fixed exit rates is wrong.

Predicting the exit rate difference with available proliferation rates. Now, we release the incorrect assumption (that the exit rates are fixed) and let $k=k_{pr}-k_e$ (assuming negligible death rate). The new equation is:

$$\ln\left(\frac{x_t}{y_t}\right)/t = (k_{prx}-k_{ex}) - (k_{pry}-k_{ey}) = (k_{prx} - k_{pry}) + (k_{ey}-k_{ex}).$$

We can now predict the exit rate difference ($k_{ey}-k_{ex}$) based on known proliferation rates and endpoint (4 day) ratio. Since we do not know k_{pry} at E14.5, we can compute two possible results:

Predicted exit rate differences with slow proliferation rates for E14.5:

<u>Age of Cited1 cell</u> (y)	<u>Ln(xt/yt)*1/4</u>	<u>(k_{prx} - k_{pry})</u>	<u>(k_{ey}-k_{ex})</u>	<u>Exit rate (k_y)</u>
14.5	-0.155	IF >0.465	THEN <-0.62	Then < k _{ex} -0.62
18.5	0.05	0.67 (1.17-0.5)	-0.62	k _{ex} -0.62
P0	0.25	0.67	-0.42	k _{ex} -0.42

The difference is negative because that Cited1 cells have a *slower exit rate* compared with Six2-E12.5 cells. For example, relative to E12.5 Six2 cells, E18.5 Cited1 cells proliferate slower. By the end of 4 days in culture similar numbers of E12.5 Six2 cells and E18.5 Cited1 cells stay in the niche. Therefore, E18.5 Cited1 cells must have a slower exit rate compared with Six2-E12.5 cells. Short et al reached the same conclusion (recall Six2 cells have a subpopulation that has been induced, whereas Cited1 cells do not).

What happens to Cited1 cells over time?

The proliferation rate of E14.5 Cited1 cells determines the conclusion. If these cells proliferate slowly enough (CCT > about 1 day), then their proliferation rate is small (<0.705 day⁻¹). In this case, $(k_{prx} - k_{pry}) > 0.465$ (=1.17- 0.705). The exit rate difference will therefore be small (<-0.62). In this case, the predicted exit rate increases with age as Cited1 cells grow older (**monotonous increase in Cited1 exit rate/age**).

We think this rate is less likely than a faster rate (CCT < 1day). In this case, the observed ratio will indicate that E14.5 Cited1 cells exit faster than E18.5 Cited1 cells, which exit slower than P0 Cited1 cells (**non-monotonous change in Cited1 exit rate/age**). Interestingly, Short et al (Figure 6F) extrapolated exit rates of Six2 cells based on the calculated vs. observed numbers of cells in the niche and find that exit rates may slow between E12.5 and E17.5 and accelerate between E17.5 and P3.

The overall conclusions from all these analysis are:

1. It is incorrect to assume identical exit rates for all Cited1 cells.
2. Cited1 cells increase their exit rates when they grow older, the overall direction of change in exit rates depends on the proliferation rates of E14.5 Cited1 cells.

Summary of analysis:

<u>Analysis</u>	<u>Input data</u>	<u>Assumption</u>	<u>Output predictions</u>	<u>Conclusion</u>
Ratio analysis-1	Ratio	All cells have identical exit rates	Proliferation rates	It is incorrect to assume identical
Ratio analysis-2	Known ratios, proliferation rates of E18.5 and P0 cells	E14.5 Cited1 cells proliferate slowly (CCT > 24hr)	Order of Exit rates	Monotonous increase of exit rates with age
Ratio analysis - 3		E14.5 Cited1 cells proliferate fast (CCT < 24hr)	Order of Exit rates	Non-monotonous exit rates with smallest exit rates for Cited E18.5 cells

Supplemental REFERENCES

Brunskill, E.W., Park, J.S., Chung, E., Chen, F., Magella, B., and Potter, S.S. (2014). Single cell dissection of early kidney development: multilineage priming. *Development* *141*, 3093-3101.

Short, K.M., Combes, A.N., Lefevre, J., Ju, A.L., Georgas, K.M., Lamberton, T., Cairncross, O., Rumballe, B.A., McMahon, A.P., Hamilton, N.A., *et al.* (2014). Global quantification of tissue dynamics in the developing mouse kidney. *Dev Cell* *29*, 188-202.